



## Hepatitis C virus polymerase–polymerase contact interface: Significance for virus replication and antiviral design



Alberto José López-Jiménez<sup>a,1</sup>, Pilar Clemente-Casares<sup>a,b,g,1</sup>, Rosario Sabariego<sup>a,c,g,1</sup>,  
María Llanos-Valero<sup>a</sup>, Itxaso Bellón-Echeverría<sup>a,2</sup>, José Antonio Encinar<sup>d</sup>, Neerja Kaushik-Basu<sup>e</sup>,  
Mathy Froeyen<sup>f</sup>, Antonio Mas<sup>a,b,g,h,\*</sup>

<sup>a</sup> Centro Regional de Investigaciones Biomédicas (CRIB), Universidad de Castilla-La Mancha, Albacete 02008, Spain

<sup>b</sup> School of Pharmacy, Universidad de Castilla-La Mancha, Albacete 02008, Spain

<sup>c</sup> School of Medicine, Universidad de Castilla-La Mancha, Albacete 02008, Spain

<sup>d</sup> Instituto de Biología Molecular y Celular, Universidad Miguel Hernández, Elche 03202, Spain

<sup>e</sup> Department of Biochemistry and Molecular Biology, Rutgers, The State University of New Jersey, New Jersey Medical School, 185 South Orange Avenue, Newark, NJ 07103, United States

<sup>f</sup> Laboratory for Medicinal Chemistry, Rega Institute for Medical Research, K.U. Leuven, Belgium

<sup>g</sup> Viral Hepatitis Study Group, Spanish Society of Virology, Madrid, Spain

<sup>h</sup> Unidad de Biomedicina, CSIC-UCLM, Spain

### ARTICLE INFO

#### Article history:

Received 20 February 2014

Revised 13 April 2014

Accepted 21 April 2014

Available online 6 May 2014

#### Keywords:

HCV

NS5B

Protein–protein interactions

Antiviral drugs

### ABSTRACT

The hepatitis C virus (HCV) replicates its genome in replication complexes located in micro-vesicles derived from endoplasmic reticulum. The composition of these replication complexes indicates that proteins, both viral and cellular in origin, are at high concentrations. Under these conditions, protein–protein interactions must occur although their role in the replication pathways is unknown. HCV RNA-dependent RNA-polymerase (NS5B) initiates RNA synthesis in these vesicles by a *de novo* (DN) mechanism. After initiation, newly synthesized dsRNA could induce conformational changes that direct the transition from an initiating complex into a processive elongation complex. In this report, we analyze the role played by NS5B–NS5B intermolecular interactions controlling these conformational rearrangements. Based on NS5B protein–protein docking and molecular dynamics simulations, we constructed mutants of residues predicted to be involved in protein–protein interactions. Changes at these positions induced severe defects in both the activity of the enzyme and the replication of a subgenomic replicon. Thus, mutations at the interaction surface decreased both DN synthesis initiation and processive elongation activities. Based on this analysis, we define at an atomic level an NS5B homomeric interaction model that connects the T-helix in the thumb subdomain of one monomer, with the F-helix of the fingers subdomain in other monomer. Knowing the molecular determinants involved in viral replication could be helpful to delineate new and powerful antiviral strategies.

© 2014 Elsevier B.V. All rights reserved.

### 1. Introduction

The phosphoryl transfer reaction of all nucleic acid polymerases is catalyzed by a two-metal ion mechanism (Steitz, 1999). In this model, the correct structural conformation must be maintained

during the replicative process to promote the formation of the phosphodiester bond (Steitz, 1999). RNA-dependent RNA-polymerases (RdRPs) catalyze the phosphoryl transfer reaction between ribonucleotides in an RNA template-dependent fashion (Ng et al., 2008). This step is critical during the replicative cycle of positive-strand RNA viruses (RNA(+)), including those infecting humans, and therefore is a key target to develop new antiviral agents (Ferrer-Orta et al., 2006). Viral and cellular proteins that together form still poorly understood replication complexes (RCs) perform RNA virus replication. The viral replication machinery is located on intracellular membranes to both increase the efficiency of replication and to protect the RNA intermediate from cellular defences (Denison, 2008). Like other RNA(+) viruses, hepatitis C

\* Corresponding author at: Centro Regional de Investigaciones Biomédicas (CRIB), Universidad de Castilla-La Mancha, Albacete 02008, Spain. Tel.: +34 967 599 200; fax: +34 967 599 360.

E-mail address: [Antonio.Mas@uclm.es](mailto:Antonio.Mas@uclm.es) (A. Mas).

<sup>1</sup> These authors contributed equally to this work.

<sup>2</sup> Present address: EMBL Grenoble, BP 181, 6 rue Jules Horowitz, 38042 Grenoble Cedex 9, France.



alteration of the conformation of the fingertips (Mosley et al., 2012). Additionally, the template channel, the entry site for the incoming nucleotide and exit channel for the newly synthesized dsRNA, can be positioned in this crystal structure without significant changes to the  $\Delta 1$  loop. When structures of NS5B in the apo and binary complex are compared, the greatest structural change involves the thumb subdomain (Fig. 1B). Specifically, the HCV NS5B–dsRNA structure shows a dramatic rearrangement of loop residues 397–405, which connects the primer buttress helix with the primer grip helix, as well as movement of several helices in the thumb domain, including the helix T (Mosley et al., 2012). Interestingly, residue His502 has been shown to be involved in intermolecular NS5B–NS5B interactions (Bellon-Echeverria et al., 2010; Qin et al., 2002; Wang et al., 2002). The structural determinants for these interactions remain elusive, although some findings point towards head-to-tail contacts which involve elements from fingers and thumb subdomains (Clemente-Casares et al., 2011; Wang et al., 2002). Polymerase–polymerase interactions have been related to polymerase function in the RNA(+) poliovirus (Hobson et al., 2001; Lyle et al., 2002; Pata et al., 1995; Spagnolo et al., 2010). Similarly, HCV NS5B–NS5B interactions have been related to its RdRP activity, and have been proposed to be potential targets for some non-nucleoside inhibitors directed against NS5B (Bellon-Echeverria et al., 2010; Biswal et al., 2006; Clemente-Casares et al., 2011; Gu et al., 2004; Love et al., 2003; Qin et al., 2002; Wang et al., 2002).

With these antecedents, we have proposed a model for NS5B–NS5B interactions, and defined the amino acid residues that play a key role in these contacts. We have studied the contribution of these residues towards NS5B RdRP activity and its RNA synthesis ability, both *in vitro* and *in vivo*. We have also tested the effect of these residues on DN initiation and primer extension (PE) activities of HCV NS5B. Based on our data, we define at a molecular level the contact surface between two HCV NS5B monomers. Importantly, the NS5B–NS5B interaction surface helps to understand the molecular mechanisms involved in efficacy and resistance of some non-nucleoside antiviral drugs directed against HCV NS5B as well as defines itself as a target for new antiviral drugs.

## 2. Material and methods

### 2.1. NS5B $\Delta 21$ polymerase, mutants and plasmid construction

The plasmid containing the gene-encoding region of HCV NS5B from genotype 1 with a deletion of 21 aa at the C-terminal end (NS5B $\Delta 21$ ) was kindly provided by Dr. Nyanguile (Pauwels et al., 2007). This polymerase (pJ4-HC strain) was mutated to introduce changes at positions R114, E128, D129, E437, E440, and H502. Previously obtained construct (from other studies) with the desired point mutations in NS5B were digested with the restriction enzymes KpnI and StuI, and the DNA fragments were ligated into the final plasmids. For cell culture experiments, the I389/NS3–3'/LucUbiNeo-ET replicon, kindly provided by Dr. Bartenschlager, was used (Frese et al., 2003). Mutations of the NS5B sequence (E128A, D129A, D220A and H502A) were performed by directed mutagenesis using the oligonucleotides described in Table S2 and the Quikchange Lightning Site-Directed Mutagenesis kit (Agilent Technologies, Madrid), following the manufacturer's instructions. All constructs were verified by DNA sequencing.

### 2.2. Protein expression and purification

Proteins used in this study were overexpressed and purified as previously reported (Bellon-Echeverria et al., 2010) in an AKTA FPLC (GE Healthcare). Aliquots of the purest and most concentrated

protein samples were adjusted to 50% glycerol and stored at  $-80^{\circ}\text{C}$  until use. All purification processes were followed by SDS–PAGE and Coomassie brilliant blue staining. Protein was quantified by SDS–PAGE gel imaging and protein determination using the Bradford assay.

### 2.3. *In vitro* RdRP and single-round replication assays

RNA polymerase assays were performed using the symmetric substrate LE-19 (sequence 5' UGUUAUAAUAAUUGUAUAC 3'), which is capable of both primer-extension and DN initiation (Fig. 1C). Except when indicated otherwise, LE-19 RNA was pre-incubated for 15 min in a reaction mixture containing 20 mM MOPS, pH 7.3, 5 mM  $\text{MnCl}_2$ , 35 mM NaCl, 100 nM NS5B and 500  $\mu\text{M}$  GTP. Reactions were started by adding 100  $\mu\text{M}$  ATP and UTP and 1  $\mu\text{Ci}$   $\alpha$ [ $^{32}\text{P}$ ]CTP (3000 Ci mmol, PerkinElmer Life Sciences). In addition, samples for single-round analysis were supplemented with 200  $\mu\text{g}/\text{ml}$  heparin after pre-incubation. Reactions were carried out in a final volume of 10  $\mu\text{l}$ . Reactions were stopped using EDTA/formamide loading buffer at different times as indicated in each experiment. Products were resolved using denaturing polyacrylamide (23% PAA, 7 M urea) gel electrophoresis. Gels were exposed to phosphorimager screens and scanned with Typhoon (Molecular Dynamics). Alternatively, X-ray autoradiography films (Amersham Hyperfilm ECL) were used. Quantification was performed from samples derived from experiments done and resolved by gel electrophoresis in parallel. Quantification of band intensities was carried out on a phosphorimager employing ImageQuant software (GE Healthcare).

### 2.4. Protein–protein docking and Molecular dynamics

The publicly available X-ray crystal structure of the apo-form of the HC-J4 RNA polymerase (1NB4) (O'Farrell et al., 2003) was obtained from the Protein Data Bank (Berman et al., 2000). The ClusPro Server (Comeau et al., 2004a,b; Kozakov et al., 2006, 2010) was used for re-docking NS5B without pre-established interaction residues. The output PDB files were used to calculate the binding energy of the generated complexes, removing clashes (using the strongest van der Waals parameters) with FoldX (Schymkowitz et al., 2005). The dimer with the best-predicted interaction energy was used in the subsequent molecular dynamics (MD) analysis. The complex was prepared using the tleap program in AMBER10 (Salomon-Ferrer et al., 2013). The parameter set used was the biomolecular force field ff99bsc0 (Perez et al., 2007). The complex was soaked in a rectangular box of TIP3P water molecules with a margin of 12 Å along each dimension.  $\text{Cl}^-$  ions were added to neutralize the system. This yielded about 170,000 atoms for the system. The solvated complex was equilibrated by carrying out a short minimization, consisting of 50 ps of heating and 50 ps of density equilibration with weak restraints on the complex, followed by 500 ps of constant pressure equilibration at 300 K. All simulations were run with shake on hydrogen atoms, a 2 fs time step, and langevin dynamics for temperature control. Production phase of the simulation was carried out using the same conditions as during the previous equilibration, and lasted a total of 2 ns with coordinates being recorded every 10 ps. In order to calculate interaction energy and solvation free energy for the complex, both MM/GBSA and MM/PBSA were used as described in Gohlke and Case (2004).

### 2.5. *In vitro* transcription, electroporation and colony formation

After digestion with ScaI, the replicon DNAs (WT and mutated variants) were extracted with phenol–chloroform to remove RNase activity. The *in vitro* transcription was performed with 1  $\mu\text{g}$  of

digested DNA and the Megascript T7 kit (Ambion), following the manufacturer's instructions. The reaction was incubated for an additional 2 h at 37 °C after supplementation with 40 U of T7 RNA pol (Ambion). The RNA obtained was purified with the MegaClear kit (Ambion), quantified, and stored at –80 °C until use.

The Huh-7 Lunet cell line employed in this study was kindly provided by R. Bartenschlager (Institute for Virology, Johannes-Gutenberg University, Mainz, Germany). Cells were electroporated with transcribed RNA from WT replicon or replicons with NS5B mutations E128A, D129A, and H502A, using Electrobuffer kit (Cell projects, Iberlabo, Madrid, Spain), in accordance with the manufacturer's instructions. Briefly, exponentially growing cells were harvested and washed with electroporation medium. Four micrograms replicon RNA plus 6 µg of carrier Huh-7 RNA (Huh-7 total RNA) were mixed with the electroporation medium and added to an aliquot of  $4 \times 10^6$  cells. The cell suspension was transferred to a cuvette (Bio-Rad Laboratories, Madrid, Spain) and pulsed once with Gene Pulser II (Bio-Rad; settings: 975 µF; 270 V). After electroporation,  $2 \times 10^6$  (undiluted sample),  $2 \times 10^5$  (1:10 dilution), and  $1 \times 10^5$  (1:20 dilution) cell suspensions were seeded in Petri dishes containing Dulbecco's modified Eagle's medium (DMEM) (Sigma–Aldrich Química, Madrid, Spain) with 10% fetal bovine serum (Hyclone, Fisher Scientific, Madrid, Spain), supplemented with 1 M HEPES (Sigma), 1% glutamine, non-essential amino acids and antibiotics (Lonza, Madrid, Spain) and cultured at 37 °C in 5% CO<sub>2</sub> incubator. Twenty-four hours later, the DMEM culture medium was replaced with fresh medium containing G418 (Labclinics, Barcelona, Spain), and then refreshed twice per week for three weeks, after which colony quantification was performed by crystal violet staining.

### 3. Results

#### 3.1. HCV NS5B is a cooperative polymerase

Previously, we and others have shown that ionic strength drives the transition of HCV NS5B from monomeric to oligomeric state (Bellon-Echeverria et al., 2010; Cramer et al., 2006). Furthermore, we have determined that a NaCl concentration range from 25 mM to 100 mM was optimal for HCV NS5B RdRP activity (Clemente-Casares et al., 2011). Based on these premises, we analyzed the DN and PE activities of HCV NS5B as a function of its concentration at low (35 mM) and high (100 mM) NaCl concentration. These experiments were done with template LE19 in the presence of GTP (products from both DN initiation and PE activities expected) or absence of GTP (only PE products expected) (Fig. 1C). Representative data for WT NS5B DN initiation and PE activities at 35 mM NaCl concentration are shown in Fig. 2A and B, respectively, and its quantification is represented in Fig. 2C. In agreement with the results obtained by Kao and colleagues (Chinnaswamy et al., 2010), we observed an exponential increase in the DN initiation and PE products (Fig. 2C, continuous lines) by WT NS5B at 35 mM NaCl concentration, which supports an oligomeric state of NS5B (Bellon-Echeverria et al., 2010; Cramer et al., 2006). This increase was more pronounced for DN activity. We adjusted the graphics obtained for WT protein to a sigmoidal curve and calculated the Hill coefficient from these data as described previously (Clemente-Casares et al., 2011). This yielded a Hill coefficient of  $6.8 \pm 1.8$  for DN synthesis, thus indicating strong cooperativity, as opposed to somewhat diminished cooperativity for PE activity, as indicated by a Hill coefficient of  $1.8 \pm 0.75$ . When the ionic strength was increased to 100 mM NaCl (Fig. 2C, dashed line), the DN activity drastically decreased (Fig. 2C, squares and dashed line). At the highest NaCl concentration tested, the curve for PE was almost coincident to the curve obtained for DN (Fig. 2C, triangles and dashed line). This result confirms NS5B's

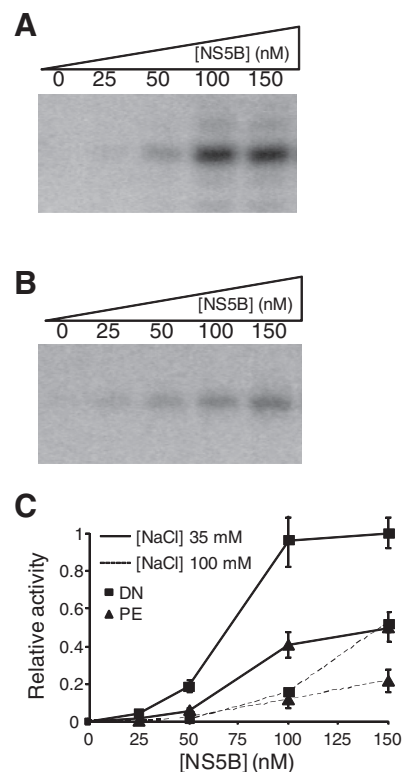


**Fig. 2.** HCV NS5B is a cooperative enzyme. (A–C). NS5B titration reactions. *De novo* (A) and primer extension (B) products obtained by WT NS5B at increasing concentrations of NS5B and at 35 mM NaCl concentration. (C) Effect of ionic strength on NS5B titrations. Relative DN and PE activities at increasing concentrations of WT NS5B protein and at indicated NaCl concentrations are shown. All reactions were carried out for 15 min (Fig. S1). Squares represent DN activity values whereas triangles represent PE products. Solid and dashed lines correspond to 35 mM and 100 mM NaCl concentration, respectively. Values correspond to the mean and SD of at least three independent experiments.

DN cooperativity, and PE to a lesser extent, are dependent on ionic strength.

In the next experiment, we included heparin in the reactions to function as a trap, and allowing only a single cycle of RNA polymerization. A schematic diagram of the experiment is depicted in Fig. 3A and results are presented in Fig. 3B and C. In the absence of heparin, when multiple cycles of RNA polymerization were allowed (Fig. 3B, lanes 1–3), DN activity was almost stable or even increased depending on the pre-incubation conditions, such as, in the absence of nucleotides (Fig. 3B and C, lane 1) or presence of GTP (the first nucleotide, Fig. 3B, lane 2, and Fig. 3C, lane 3) or GTP + UTP (the nucleotides that will be part of the initial dinucleotide, Fig. 3B, lane 3 and Fig. 3C, lane 5). By contrast, the PE product decreased when the reaction was pre-incubated with nucleotides (Fig. 3B, lanes 2 and 3, and Fig. 3C, lanes 4 and 6). When the reaction was performed in the presence of heparin and without nucleotides during the preincubation period, only the PE product was obtained (Fig. 3B, lane 4, and Fig. 3C, lane 8). This result was not surprising, since only this kind of product can be synthesized when (i) GTP is lacking in the preincubation reaction, and (ii) heparin functions as a NS5B trap, thereby preventing any new synthesis when GTP and the other nucleotides are added after the pre-incubation phase (Fig. 3B lane 4, and Fig. 3C, lane 8). Pre-incubation with GTP in the presence of heparin by contrast, yielded both the DN and PE products (Fig. 3B, lane 5, and Fig. 3C, lanes 9 and 10). Interestingly, when the reaction was pre-incubated with the nucleotides GTP and UTP in the presence of heparin, only DN products were obtained as shown in Fig. 3B (lane 6) and C (lane 11).

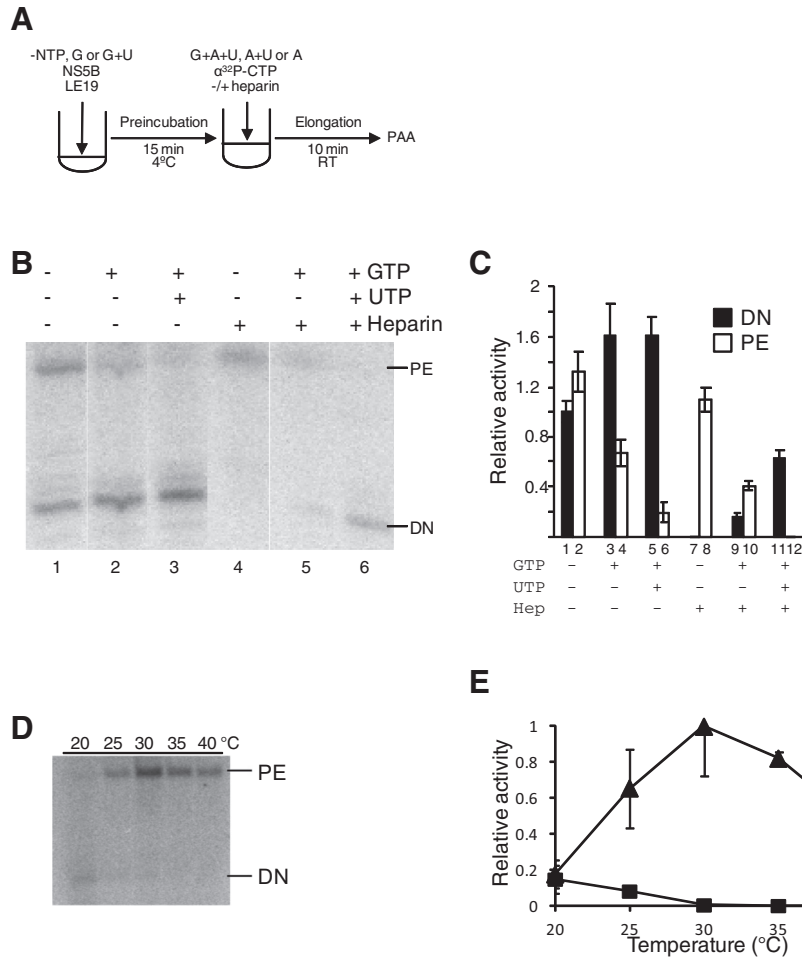


**Fig. 3.** NS5B activity in the presence of an enzyme trap. (A) Schematic representation of the one-cycle experiment. Pre-incubation was performed at 4 °C by mixing RNA template LE19 (50 nM), and NS5B (100 nM) in the reaction buffer as described in Section 2. Where indicated, this mix was supplemented with GTP or GTP and UTP, the first and the second nucleotides to be incorporated, respectively. After 15 min, the reaction was initiated by adding [ $\alpha^{32}\text{P}$ ]-CTP, the nucleotides lacking in the mix (ATP or ATP and UTP), and heparin (where indicated). Reactions were carried out for 10 min at room temperature, quenched with stop dye, heated at 95 °C, and the products were resolved by denaturing polyacrylamide electrophoresis. (B) Reaction products obtained in the absence (lanes 1–3) or presence (lanes 4–6) of the enzyme trap heparin. GTP and UTP indicate pre-incubation conditions whereas heparin refers to its absence or presence as a trap during the reaction. DN (*de novo* synthesis) and PE (primer extension) products are indicated. (C) One cycle reaction quantification. Histogram showing relative activities of the NS5B polymerase obtained in B (normalized to line 1). Black bars correspond to DN products and white bars to PE. Pre-incubation conditions (absence or presence of GTP or GTP and UTP) and the status of heparin in the reaction are indicated at the bottom. Values correspond to the mean and SD of at least three independent experiments. (D) Effect of temperature on the “one-cycle” reaction products. Reactions were preincubated in the presence of GTP to obtain PE and DN products. Temperature of the reactions is as indicated at the top. (E) Representation of activity values as a function of the temperature by quantification of the products shown in D. *De novo* synthesis is represented by a solid line and squares, and PE by a solid line and triangles. Values are the mean and SD of at least three independent experiments. Band intensities were measured on a phosphorimager (GE Healthcare) employing ImageQuant software.

The one-cycle conditions described above allowed us to explore the effect of reaction temperature on DN or PE activities separately. Under these one-cycle conditions, we tested the formation of DN and PE products at a range of temperatures in the absence or presence of GTP + UTP during the pre-incubation period (Fig. 3D and E). At the lowest temperature tested (20 °C), low and almost equivalent levels of DN and PE products were observed. At 25 °C, PE products were 6-fold more prevalent than DN products. PE product formation peaked at 30 °C, and then gradually decreased at 35 °C and 40 °C. DN products were virtually non-existent at temperatures of 30 °C and higher. Based on this data, we conclude that DN initiation reaction in our experimental setting is more sensitive to temperature than PE and does not take place at temperatures of 30 °C or higher (Fig. 3E).

### 3.2. WT RdRP activity can be complemented in trans

If protein–protein contacts play a role in modulation of RNA-polymerase activities, then it should be possible to regulate these

activities by adding mutants with a lethal defect in activity (e.g. D220A). Functional polymerase–polymerase contacts of the poliovirus 3D protein have been previously demonstrated using this strategy (Spagnolo et al., 2010). We followed a similar approach to investigate the DN and PE activities of wild type HCV NS5B in the absence or presence of increasing concentrations of the lethal mutant D220A using LE19 as a template. To perform this experiment, we chose a WT NS5B concentration (100 nM) which yielded very low amounts of product, and determined whether supplementation of wild type NS5B polymerase with catalytically inactive NS5B could create functional polymerase oligomers (Fig. 4). When the lethal mutant was present in the reaction, cooperation between WT and D220A enzymes was readily detected as an increase in the amount of DN and PE products (Fig. 4A and B). To determine the specificity of this *trans* complementation, we constructed and assayed the double mutant D220A/H502A (DH), which neither shows activity nor NS5B–NS5B interactions (Bellon-Echeverria et al., 2010). In this case, the amount of DN and PE products decreased as the concentration of DH increased

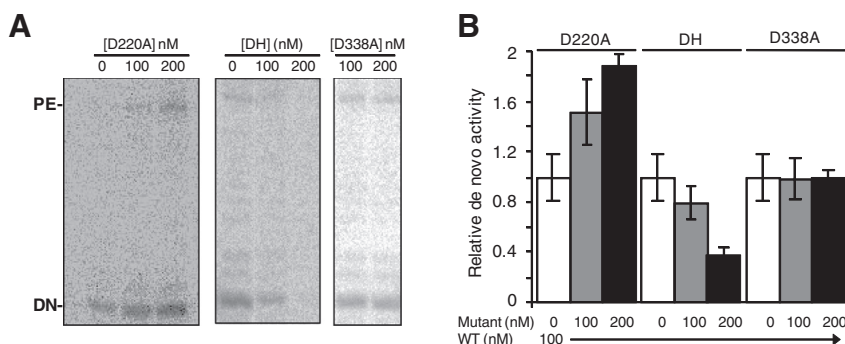


**Fig. 4.** *Trans* complementation of NS5B RNA-polymerase activity by supplementation with lethal mutants. (A) Effect of the presence of lethal mutants on NS5B activity. RNA-polymerase reactions of WT NS5B (100 nM) using LE19 as a template were complemented *in trans* by adding increasing concentrations (100 nM and 200 nM) of an NS5B mutant that is lethal for activity (D220A), an NS5B mutant that is lethal for both activity and NS5B–NS5B interactions (D220A/H502A, DH), and a foot-and-mouth-disease virus 3Dpol mutant that is lethal for activity (D338A). Products from primer extension (PE) and *de novo* initiation (DN) activities are shown. (B) Quantification of DN *trans*-complementation reactions. Histogram showing relative activity of the RNA-polymerase *de novo* activity obtained in A. Bars represent DN products obtained in the absence (white) or presence of 100 nM (gray) or 200 nM (black) mutant proteins, which are specified at the top. Values correspond to the mean and the SEM of at least three independent experiments. Reactions were carried out for 15 min (Fig. S1). Band values were obtained by using the ImageQuant software as described in Section 2.

(Fig. 4A and B). The specificity of the reaction was lastly tested by performing the experiment with an unrelated lethal mutant (D338A) of the 3D polymerase from the foot-and-mouth-disease virus (FMDV) (Ferrer-Orta et al., 2009, 2004). In this experiment, the levels of the DN and PE products were unaltered despite the presence of the lethal FMDV polymerase. These results thus demonstrate that NS5B polymerase function can be complemented *in trans* by a catalytically inactive NS5B mutant, and this effect is lost in the presence of a NS5B mutant lethal for both activity and NS5B–NS5B interactions.

### 3.3. Molecular dynamics

Fingers and thumb domains in NS5B have been previously related to NS5B–NS5B interactions (Clemente-Casares et al., 2011; Wang et al., 2002). These interactions may be responsible for the cooperative mode of RNA synthesis shown by NS5B. In order to search for a more energetically favorable pose for this interaction, we performed a first round of protein–protein docking analysis. Results were obtained without applying any restrictions to the model. Interestingly, among the best-scoring results, interactions between helices F and T appeared most likely. After this, a short molecular dynamics simulation (2 ns) in explicit solvent was carried out to obtain a relaxed model, and MM/PBSA calculations were performed to determine the NS5B dimerization energy. The energetically most favourable model with a total free energy of binding of  $-102 \text{ kcal mol}^{-1}$  and a calculated buried surface area of  $961.9 \text{ \AA}^2$  is presented in Fig. 5. Energy contributions to the mean binding energy for the 250 snapshots (Table S1) were in accordance with results obtained for other relevant protein–protein interactions such as Ras–Raf (Gohlke and Case, 2004) and the human immunodeficiency virus protease (Wang and Kollman, 2000). Several residues from both monomers are present in the model of a NS5B homodimer comprising of interacting amino acids from helices F (part of the fingers domain) and T (part of the thumb domain), as well as residues from the  $\beta$ -loop and fingertips (Fig. 5A). The majority of these residues are fully conserved among different genotypes. Monomer A contributes the conserved residues R114, H118, D125, E128, and D129 from helix F, as well as residues F101, P265, and Y276. Monomer B contributes the conserved amino acids I23, P25, and R32 from the fingertips, E437, and E440 from the  $\beta$ -loop, and R503, and R505 from helix T. These residues establish interactions mainly by ionic interactions. Only

residues F101, P265, and Y276 are involved in hydrophobic interactions (Fig. 5B).

### 3.4. RNA-polymerase activity of NS5B bearing mutations located at the contact surface

Taking into account the favoured energy model and our previous results (Bellon-Echeverria et al., 2010; Qin et al., 2002) we constructed mutants of residues from helices F and T. Specifically, positions E128, D129, and H502 were mutated to alanine, E437 and E440R mutated to arginine and position R114 was mutated to glutamate. To test the effect of these mutations on the cooperativity of DN RdRP activity, we performed polymerase assays at increasing concentrations of the mutant proteins. In Fig. 6A, we depict the increase in DN initiation activity as a function of NS5B protein concentration. For the WT NS5B, its DN activity exhibited a 5-fold increase as its concentration increased from 50 nM to 100 nM, and remained steady upto 150 nM of HCV NS5B protein concentration. This sigmoidal curve allowed us to calculate the Hill coefficient as reported for Fig. 2C. By contrast, R114E mutant exhibited linearity for DN product formation at all NS5B protein concentrations tested. The other mutants exhibited relatively poor DN activities compared to the WT or R114E NS5B. Of these, E128A, D129A, and E437R exhibited lower than 15% DN activities relative to the WT NS5B (Fig. 6A), while E440R and H502A displayed  $\sim 30\%$  and 40% DN activity, respectively relative to WT NS5B at the highest protein concentration tested (Fig. 6A). This data indicates that mutations at the contact surface of NS5B polymerase results in impairment of DN initiation activity of the protein, albeit to different extents depending on the contact residue mutated.

Since DN initiation activity was diminished in the surface mutants (Fig. 6A), we were curious to know the status of PE activity and the transition from initiation to elongation in these mutants. With this objective, we investigated and analyzed the ratio of DN to PE activities of the different mutants, and compared them to the value obtained for the WT protein. Towards this end, we performed experiments in the absence or presence of GTP to compare the amount of product obtained from DN activity (plus GTP) to that of PE (minus GTP) (Fig. 6B). Mutants R114E, E437R, and E440R displayed very low levels of PE and they were not included in this analysis. Mutants E128A, D129A, and H502A, showed lower DN and PE activities than WT NS5B (Fig. 6B). The diminution was more pronounced for PE than for DN initiation, and this manifested in an increase in their DN/PE ratios (Fig. 6B).

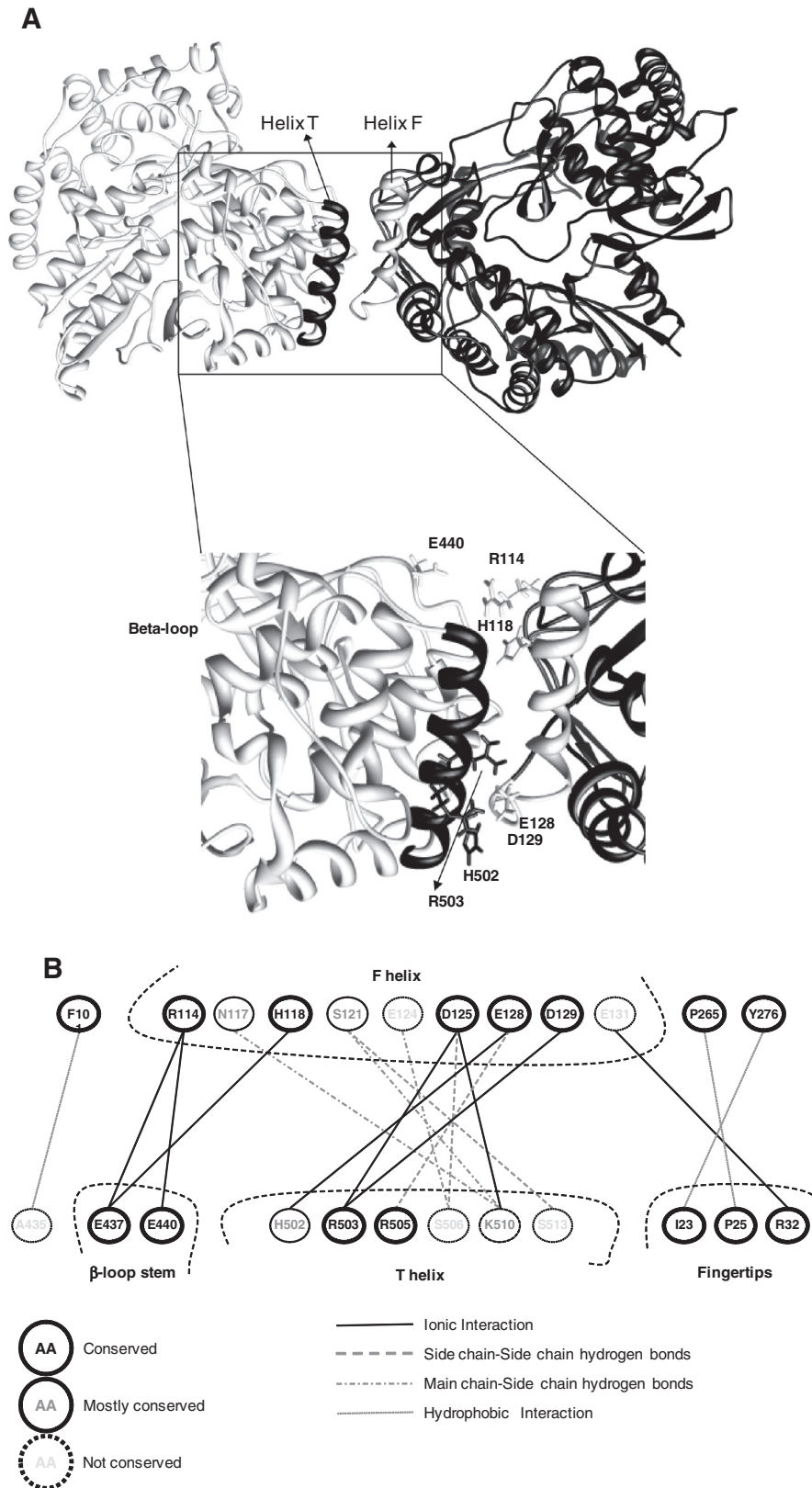


**Fig. 5.** Molecular modeling and protein docking. (A) Model showing the energetically most favorable dimer. In white is shown one monomer and in black the other. Helix T from monomer in white is colored black, and helix F from black monomer is colored in white. A zoom of the interaction surface is shown in the lower part of the figure, showing the side chains of the most important residues forming part of the interaction surface as well as the  $\beta$ -loop of the monomer in white. (B) Scheme showing the most energetically plausible NS5B–NS5B interactions. The upper part corresponds to domains and amino acids from one monomer and the lower part to an interactive second monomer. The most important NS5B domains such as fingertips, helices, and the  $\beta$ -loop stem are indicated. Interactions corresponding to ionic side chain–side chain hydrogen bonds, main chain–side chain hydrogen bonds, and hydrophobic interactions are as indicated. Encircled black amino acid position numbers indicate residues that are totally conserved among genotypes, encircled gray amino acid positions indicate residues that are mostly conserved among genotypes, dashed-encircled gray amino acid positions indicate residues that are not conserved. Ionic protein–protein interactions were studied with the Protein Interaction Calculator (PIC) web server (Tina et al., 2007).

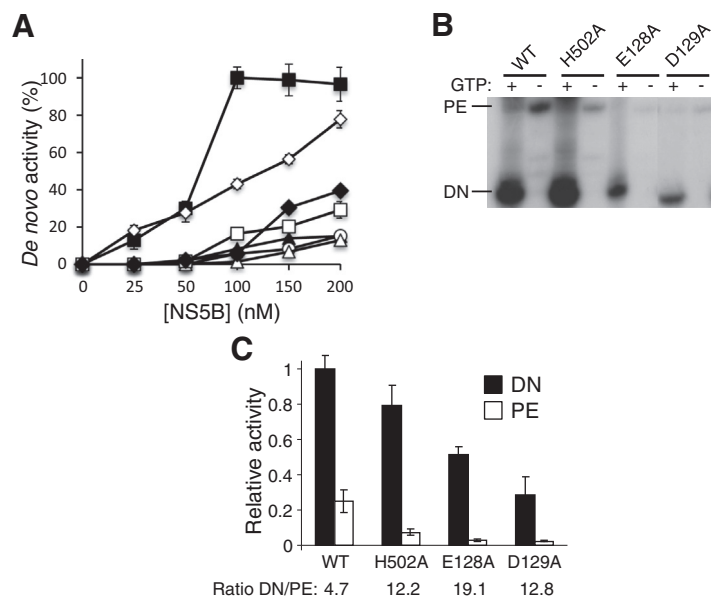


**Fig. 6.** Effect of mutations located at the NS5B interaction surfaces on polymerase activity. (A) NS5B activity of indicated mutants. Effect of increasing concentration of NS5B WT (squares) and mutants R114E (open diamonds), E128A (filled triangles), D129A (open circles), E437R (open triangles), E440R (open squares), and H502A (filled diamonds) on the synthesis of *de novo* initiation products. Reactions carried out by the wild type NS5B were stopped after 15 min whereas reactions with mutant proteins were stopped after 55 min (Fig. S1). The amount of *de novo* product (expressed as product·min<sup>-1</sup>) synthesized by each enzyme was plotted against increasing concentrations of the NS5B proteins. (B) Quantification of mutants' activities. Histogram showing relative activity of the RNA-polymerase activities of WT, E128A, D129A, and H502A. The black and white bars represent the DN and PE products, respectively, and values correspond to the mean and SEM of at least three independent experiments. The DN/PE ratios are indicated at the bottom.

### 3.5. Effect of mutations in NS5B–NS5B contact sites on cell colony formation in Huh7 Lunet cells

To determine the effects of mutations in NS5B in a biologically more relevant context, mutations E128A, D129A, and H502A were engineered into the replication-competent subgenomic HCV RNA. Plasmids were linearized, RNA was obtained by *in vitro* transcription, and *in vitro* transcripts were used to transfect Huh7 Lunet cells by electroporation followed by selection for G418 resistance (Lohmann et al., 1999a). Replication of the subgenomic HCV replicon RNA in Huh7 Lunet cells results in expression of neomycin phosphotransferase, which renders Huh7 Lunet cells resistant to the antibiotic G418 (Lohmann et al., 1999a). Three different conditions were analyzed in triplicate (2 μg RNA, and 1/10 and 1/20 dilutions thereof) as described in Materials and Methods. The results showed a moderate effect of the E128A mutation, and a severe or even lethal effect of mutations D129A and H502A (Fig. 7). By comparing the transfections with undiluted and diluted RNA, we could infer that the colony forming ability of H502A subgenomic replicon decreased by 10–20-fold with respect to WT, whereas mutation D129A was lethal. These results indicate that some positions at the surface of the polymerase, which could form part of the putative NS5B–NS5B contact sites, may be important for the replication of the HCV subgenomic replicon in Huh7 Lunet cells.

## 4. Discussion

Viruses have different strategies to initiate genome replication. HCV initiates its genome synthesis *in vitro*, and presumably *in vivo*, by a DN mechanism requiring the replicase, template and triphosphate nucleotides (Luo et al., 2000; Zhong et al., 2000). The structural requirements for DN initiation have been broadly described for the bacteriophage ϕ6 RNA-dependent RNA polymerase (Butcher et al., 2001). In this model, some domains of the RNA polymerase act as a platform where the first two nucleotides are

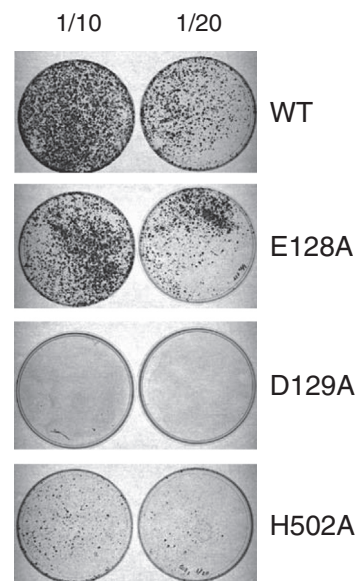


**Fig. 7.** Effect of interaction mutations in the replication of a subgenomic replicon. *In vivo* analyses using the subgenomic replicon system in the Huh7 Lunet cell line are shown. Mutants tested were E128A, D129A, and H502A, and they were compared to WT replicon. Huh-7 cells were electroporated with 1 μg of the corresponding p1389/NS3–3'/LucUbiNeo-ET replicon RNA and then grown in DMEM medium containing G418 until colonies were visible. Three different transfected cell concentrations were used (see Section 2) and shown are the ten-fold and twenty-fold diluted cell suspensions.

positioned in the correct orientation to form the phosphodiester bond and generate the dinucleotide. After completion of the first phosphodiester bond, protein domains responsible for initiation must be rearranged to allow the accommodation of the primer-template RNA (Butcher et al., 2001). HCV NS5B domains acting as the initiation platform have also been described by extensive

mutational and biochemical analyses (Ranjith-Kumar and Kao, 2006). The  $\beta$ -loop and C-terminal domain have been pinpointed as the structural elements responsible for DN initiation of HCV RNA (Harrus et al., 2010; Hong et al., 2001; Ranjith-Kumar et al., 2002). Both domains must be accurately positioned to allow NS5B to synthesize the dinucleotide. Moreover, both domains have to be relocated thereafter to allow NS5B to elongate in a template-dependent manner the newly synthesized short primer.

Consistent with previous observations, we have demonstrated cooperativity in RNA synthesis (Figs. 2 and 3) (Bellón-Echeverría et al., 2010; Clemente-Casares et al., 2011; Chinnaswamy et al., 2010; Gu et al., 2004; Qin et al., 2002; Wang et al., 2002). We have also shown that low levels of wild type NS5B activity can be enhanced by *trans*-complementation with the D220A lethal mutant, but this activity is decreased if the lethal mutant also carried the H502A mutation (mutant DH), which abrogates NS5B–NS5B interaction (Fig. 4). By using molecular dynamics and *in silico* docking we propose a model in which helix F residues from one NS5B molecule stabilize the  $\beta$ -loop, fingertips, and T helix from the thumb subdomain of a second molecule, to ensure DN initiation (Figs. 5 and 8). Thus, residues R114, E128, D129, E437, E440, and H502 among others would be involved in these protein–protein interactions. These NS5B interactions can be supposed to be pangenomic, although genotype 2a harbors serine at position 502 and 510 of NS5B. Previously, we have demonstrated that NS5B from HCV genotype 2a exhibited a lower interaction level than that from genotype 1b (Clemente-Casares et al., 2011). Furthermore, the genotype 2a NS5B mutation E125K could compensate at least in part the deleterious effect of H502S and K510S, although this hypothesis needs to be further validated experimentally. Although, the position of these interacting surfaces are located far from the active site, as well as from the rNTP and template channels (Fig. S3), nonetheless the mutations introduced at these positions greatly affect RNA synthesis (Fig. 6). Previous studies have shown the importance of NS5B homomeric interactions for HCV replication and infection (Bellón-Echeverría et al., 2010; Clemente-Casares et al., 2011; Cramer et al., 2006; Chinnaswamy et al., 2010; Gu et al., 2004; Love et al., 2003; Qin et al., 2002; Wang et al., 2002). These findings suggest that NS5B–NS5B interactions may modulate RNA synthesis both during initiation and elongation steps, as well as the transition from initiation to elongation. Of note, when replicated in Huh7 Lunet cells, mutants described in this study rendered *in vivo* subgenomic replicons with moderate to severe defects (Fig. 7) indicating that these positions are physiologically relevant in the context of virus replication.

Recent findings have indicated that I405 in HCV NS5B might be responsible for the high DN initiation efficiency shown by the JFH1 isolate (Scrima et al., 2012; Schmitt et al., 2011). The side chain of this amino acid possibly stabilizes the  $\beta$ -loop by intra-molecular interactions in a position that favours DN synthesis (Fig. 8). However, in the majority of the isolates described to date, a valine instead of isoleucine is present at this position (Waheed et al., 2012). Moreover, residues E18, I405, W397, and H428, among others, also interact with the  $\beta$ -loop or fingertips to maintain the internal structure that is needed for the correct positioning of initiation factors (mainly nucleotides, template, and divalent cations) (Chinnaswamy et al., 2008; Simister et al., 2009). According to our results, inter-molecular interactions between helix F from the fingers subdomain of one NS5B molecule and helix T from the thumb subdomain of a second molecule could play the same role as I405 in the intra-molecular model. Consistent with this hypothesis, several mutations at positions in the vicinity of the F helix in the fingers subdomain have been correlated with resistance to the site II NS5B inhibitor drug filibuvir. This drug binds to the thumb domain of NS5B and selects resistant mutations at the binding site as well as, and more intriguingly, at positions 110 and 134 in the fingers domain (Shi et al., 2009). The NS5B–NS5B interactions described in this study could be useful to understand these results.

Part of the NS5B–NS5B interaction surface overlaps with the putative allosteric GTP binding site (Bressanelli et al., 2002; Cai et al., 2005). The existence and exact function of this allosteric GTP binding site is controversial. Activation of HCV NS5B as well as other RNA(+) virus polymerases by GTP has been described previously (Chinnaswamy et al., 2010; Choi et al., 2004; Harrus et al., 2010; Lohmann et al., 1999b; Morin et al., 2012; Nomaguchi et al., 2003). GTP-driven activation of NS5B must occur at the DN initiation step because increasing concentrations of this nucleotide specifically inhibited PE activity on LE19 RNA template (Ranjith-Kumar et al., 2002). We have also shown that GTP inhibits NS5B–NS5B interaction (Bellón-Echeverría, 2011) (Fig. S2). This inhibition is dependent on the number of phosphates of the nucleoside as well as on the concentration of the triphosphate nucleotide. Similar observations have been previously reported when NS5B was resolved by gel filtration chromatography in the absence or presence of GTP (Chinnaswamy et al., 2010). Dr. Kao and co-workers also observed an increase in the thermal stability of NS5B in a GTP-concentration-dependent manner (Chinnaswamy et al., 2010). Moreover, mutations at positions R32, E128, D129, Y276, H502, and R503, which form part of the putative allosteric GTP binding site, showed severe defects in their phenotypes when

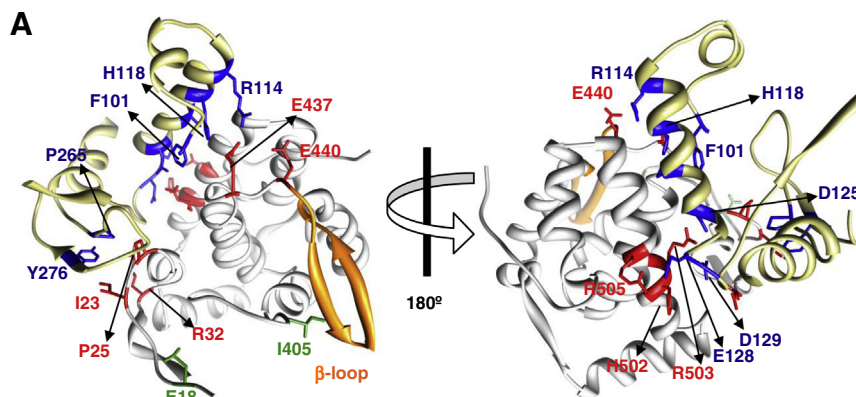


**Fig. 8.** Model of NS5B–NS5B interaction. (A) Zoom in at the interaction surface. Interacting parts of two NS5B monomers (gray and khaki) are depicted. Side chains from residues that are involved in the interaction between a monomer and its binding partner are shown in red and blue, respectively. Residues E18 and I405 are shown in green, whereas the  $\beta$ -loop is depicted in orange.

introduced in an HCV replicon (Fig. 7) (Cai et al., 2005; Ma et al., 2004; Qin et al., 2001). Some of these positions are also related to the NS5B–NS5B contacts described in this study (Figs. 5 and 8). These studies argue in favor of a closed conformation of the polymerase and GTP concentrations as among the prime regulators of DN initiation by NS5B.

NS5B–NS5B interactions described in this study (Figs. 5 and 8) do not hamper RdRP activity. The rNTP entry channel, template channel, and dsRNA exit channel described recently (Deval et al., 2007; Mosley et al., 2012) are accessible in the NS5B homodimer (Fig. S3 A–C). The NS5B residues involved in the putative interaction with NS5A (Qin et al., 2001), and postulated to be critical for NS5A binding, have also been mapped in this model (Fig. S3 D). Therefore, monomers in the complex could carry out the RNA-polymerase reaction in this scenario when NS5B interacts with itself, as the rNTP and template can gain access into the NS5B catalytic active site, and the dsRNA product can exit from it. The observed NS5B–NS5B interaction does not exclude the possibility that only some monomers are performing DN initiation, whereas other molecules could acquire the conformation for PE. Interestingly, dsRNA exit channel has been mapped at two different locations, one through the channel open by the C-terminal end movement (Mosley et al., 2012) and the other through the rNTP entry channel (Vaughan et al., 2012). Our data suggests the concurrence of both options. This may be visualized as a closed NS5B initiating by a DN mechanism the synthesis of a dsRNA comprising of a template primed with a short oligonucleotide. This dsRNA could then exit through the rNTP exit channel, get transferred to a NS5B in an open conformation where it could then get elongated and exit through the channel open by the C-terminal end movement. This paradigm however needs to be validated experimentally by using structural and biophysical approaches, and might help to clarify the structural determinants and dynamics of the HCV replication complex.

Polymerase–polymerase interactions have been previously reported for other RNA(+) viruses including poliovirus (Hobson et al., 2001; Spagnolo et al., 2010), calicivirus (Kaiser et al., 2006), and foot-and-mouth-disease virus (Bentham et al., 2012). In this study, we have shown that homomeric NS5B interactions are important both for RdRP activity and *in vivo* replication of a HCV subgenomic replicon. In addition, we have defined the surfaces involved in this interaction *in silico*, and demonstrated their importance by biochemical and cellular HCV-replication experiments. This model may explain the allosteric role of GTP in NS5B RdRP catalyzed reactions as well as the reported discrepancies of the dsRNA exit channel. In conclusion, we have described a novel strategy by which NS5B polymerase stabilizes itself in a conformation suitable for DN initiation of HCV RNA replication. Data presented in this study provides mechanistic clues as to how the HCV macromolecular replication complex may rearrange during HCV replication as well as the mechanism of some resistant mutations located far from the binding site of the drug. Furthermore, the NS5B–NS5B contacts proposed herein could be the target for new therapeutic interventions.

## Acknowledgements

We thank Elena Ruiz López for excellent technical assistance. We are indebted to Esteban Domingo, Nuria Verdager, Piet W.J. de Groot and Ricardo Sánchez Prieto for their valuable suggestions and critical reading of the manuscript. Cell line Huh7-Lunet and plasmid pI389/NS3-3'/LucUbiNeo-ET were kindly provided by Dr. Bartenschlager. Dr. Domingo is also acknowledged for providing useful reagents and for permitting us to perform some experiments in his laboratory. This work was supported by Ministerio de Ciencia e Innovación (grant number BFU2010-18767), and the Consejería

de Educación de Castilla-La Mancha (grant number PPII10-0243-6857). A.J.L.J. was supported by a pre-doctoral fellowship from Fundación para la Investigación Sanitaria de Castilla-La Mancha (grant number MOV-2008\_JI/1).

## Appendix A. Supplementary data

Supplementary data associated with this article can be found, in the online version, at <http://dx.doi.org/10.1016/j.antiviral.2014.04.009>.

## References

- Behrens, S.E., Tomei, L., De Francesco, R., 1996. Identification and properties of the RNA-dependent RNA polymerase of hepatitis C virus. *EMBO J.* 15, 12–22.
- Bellón-Echeverría, I., 2011. Analyses of factors and domains involved in the homomeric interaction of the hepatitis C virus RNA-polymerase. Medical Sciences, University of Castilla-La Mancha, Ciudad Real, Spain, p. 158.
- Bellón-Echeverría, I., López-Jiménez, A.J., Clemente-Casares, P., Mas, A., 2010. Monitoring hepatitis C virus (HCV) RNA-dependent RNA polymerase oligomerization by a FRET-based *in vitro* system. *Antiviral Res.* 87, 57–66.
- Bentham, M., Holmes, K., Forrest, S., Rowlands, D.J., Stonehouse, N.J., 2012. Formation of higher-order foot-and-mouth disease virus 3D(pol) complexes is dependent on elongation activity. *J. Virol.* 86, 2371–2374.
- Berman, H.M., Westbrook, J., Feng, Z., Gilliland, G., Bhat, T.N., Weissig, H., Shindyalov, I.N., Bourne, P.E., 2000. The protein data bank. *Nucleic Acids Res.* 28, 235–242.
- Biswal, B.K., Cherney, M.M., Wang, M., Chan, L., Yannopoulos, C.G., Bilimoria, D., Nicolas, O., Bedard, J., James, M.N., 2005. Crystal structures of the RNA-dependent RNA polymerase genotype 2a of hepatitis C virus reveal two conformations and suggest mechanisms of inhibition by non-nucleoside inhibitors. *J. Biol. Chem.* 280, 18202–18210.
- Biswal, B.K., Wang, M., Cherney, M.M., Chan, L., Yannopoulos, C.G., Bilimoria, D., Bedard, J., James, M.N., 2006. Non-nucleoside inhibitors binding to hepatitis C virus NS5B polymerase reveal a novel mechanism of inhibition. *J. Mol. Biol.* 361, 33–45.
- Bressanelli, S., Tomei, L., Rey, F.A., De Francesco, R., 2002. Structural analysis of the hepatitis C virus RNA polymerase in complex with ribonucleotides. *J. Virol.* 76, 3482–3492.
- Bressanelli, S., Tomei, L., Roussel, A., Incitti, I., Vitale, R.L., Mathieu, M., De Francesco, R., Rey, F.A., 1999. Crystal structure of the RNA-dependent RNA polymerase of hepatitis C virus. *Proc. Natl. Acad. Sci. U.S.A.* 96, 13034–13039.
- Butcher, S.J., Grimes, J.M., Makeyev, E.V., Bamford, D.H., Stuart, D.I., 2001. A mechanism for initiating RNA-dependent RNA polymerization. *Nature* 410, 235–240.
- Cai, Z., Yi, M., Zhang, C., Luo, G., 2005. Mutagenesis analysis of the rGTP-specific binding site of hepatitis C virus RNA-dependent RNA polymerase. *J. Virol.* 79, 11607–11617.
- Clemente-Casares, P., López-Jiménez, A.J., Bellón-Echeverría, I., Encinar, J.A., Martínez-Alfaro, E., Pérez-Flores, R., Mas, A., 2011. De novo polymerase activity and oligomerization of hepatitis C virus RNA-dependent RNA-polymerases from genotypes 1 to 5. *PLoS One* 6, e18515.
- Comeau, S.R., Gatchell, D.W., Vajda, S., Camacho, C.J., 2004a. ClusPro: a fully automated algorithm for protein–protein docking. *Nucleic Acids Res.* 32, W96–99.
- Comeau, S.R., Gatchell, D.W., Vajda, S., Camacho, C.J., 2004b. ClusPro: an automated docking and discrimination method for the prediction of protein complexes. *Bioinformatics* 20, 45–50.
- Cramer, J., Jaeger, J., Restle, T., 2006. Biochemical and pre-steady-state kinetic characterization of the hepatitis C virus RNA polymerase (NS5BDelta21, HC-J4). *Biochemistry* 45, 3610–3619.
- Chinnaswamy, S., Murali, A., Li, P., Fujisaki, K., Kao, C.C., 2010. Regulation of de novo-initiated RNA synthesis in hepatitis C virus RNA-dependent RNA polymerase by intermolecular interactions. *J. Virol.* 84, 5923–5935.
- Chinnaswamy, S., Yarbrough, I., Palaninathan, S., Kumar, C.T., Vijayaraghavan, V., Demeler, B., Lemon, S.M., Sacchettini, J.C., Kao, C.C., 2008. A locking mechanism regulates RNA synthesis and host protein interaction by the hepatitis C virus polymerase. *J. Biol. Chem.* 283, 20535–20546.
- Choi, K.H., Groarke, J.M., Young, D.C., Kuhn, R.J., Smith, J.L., Pevear, D.C., Rossmann, M.G., 2004. The structure of the RNA-dependent RNA polymerase from bovine viral diarrhoea virus establishes the role of GTP in de novo initiation. *Proc. Natl. Acad. Sci. U.S.A.* 101, 4425–4430.
- Denison, M.R., 2008. Seeking membranes: positive-strand RNA virus replication complexes. *PLoS Biol.* 6, e270.
- Deval, J., D'Abramo, C.M., Zhao, Z., McCormick, S., Coutsinos, D., Hess, S., Kvaratskhelia, M., Gotte, M., 2007. High resolution footprinting of the hepatitis C virus polymerase NS5B in complex with RNA. *J. Biol. Chem.* 282, 16907–16916.
- Doublie, S., Sawaya, M.R., Ellenberger, T., 1999. An open and closed case for all polymerases. *Structure* 7, R31–R35.

- Ferrer-Orta, C., Agudo, R., Domingo, E., Verdaguier, N., 2009. Structural insights into replication initiation and elongation processes by the FMDV RNA-dependent RNA polymerase. *Curr. Opin. Struct. Biol.* 19, 752–758.
- Ferrer-Orta, C., Arias, A., Escarmis, C., Verdaguier, N., 2006. A comparison of viral RNA-dependent RNA polymerases. *Curr. Opin. Struct. Biol.* 16, 27–34.
- Ferrer-Orta, C., Arias, A., Perez-Luque, R., Escarmis, C., Domingo, E., Verdaguier, N., 2004. Structure of foot-and-mouth disease virus RNA-dependent RNA polymerase and its complex with a template-primer RNA. *J. Biol. Chem.* 279, 47212–47221.
- Frese, M. et al., 2003. *J. Virol.* 84, 1253–1259.
- Gohlke, H., Case, D.A., 2004. Converging free energy estimates: MM-PB(GB)/SA studies on the protein–protein complex Ras–Raf. *J. Comput. Chem.* 25, 238–250.
- Gu, B., Gutshall, L.L., Maley, D., Pruss, C.M., Nguyen, T.T., Silverman, C.L., Lin-Goerke, J., Khandekar, S., Liu, C., Baker, A.E., Casper, D.J., Sarisky, R.T., 2004. Mapping cooperative activity of the hepatitis C virus RNA-dependent RNA polymerase using genotype 1a–1b chimeras. *Biochem. Biophys. Res. Commun.* 313, 343–350.
- Harrus, D., Ahmed-El-Sayed, N., Simister, P.C., Miller, S., Triconnet, M., Hagedorn, C.H., Mahias, K., Rey, F.A., Astier-Gin, T., Bressanelli, S., 2010. Further insights into the roles of GTP and the C terminus of the hepatitis C virus polymerase in the initiation of RNA synthesis. *J. Biol. Chem.* 285, 32906–32918.
- Hobson, S.D., Rosenblum, E.S., Richards, O.C., Richmond, K., Kirkegaard, K., Schultz, S.C., 2001. Oligomeric structures of poliovirus polymerase are important for function. *EMBO J.* 20, 1153–1163.
- Hong, Z., Cameron, C.E., Walker, M.P., Castro, C., Yao, N., Lau, J.Y., Zhong, W., 2001. A novel mechanism to ensure terminal initiation by hepatitis C virus NS5B polymerase. *Virology* 285, 6–11.
- Huang, H., Chopra, R., Verdine, G.L., Harrison, S.C., 1998. Structure of a covalently trapped catalytic complex of HIV-1 reverse transcriptase: implications for drug resistance. *Science* 282, 1669–1675.
- Kaiser, W.J., Chaudhry, Y., Sosnovtsev, S.V., Goodfellow, I.G., 2006. Analysis of protein–protein interactions in the feline calicivirus replication complex. *J. Gen. Virol.* 87, 363–368.
- Kozakov, D., Brenke, R., Comeau, S.R., Vajda, S., 2006. PIPER: an FFT-based protein docking program with pairwise potentials. *Proteins* 65, 392–406.
- Kozakov, D., Hall, D.R., Beglov, D., Brenke, R., Comeau, S.R., Shen, Y., Li, K., Zheng, J., Vakili, P., Paschalidis, I., Vajda, S., 2010. Achieving reliability and high accuracy in automated protein docking: ClusPro, PIPER, SDU, and stability analysis in CAPRI rounds 13–19. *Proteins* 78, 3124–3130.
- Lesburg, C.A., Cable, M.B., Ferrari, E., Hong, Z., Mannarino, A.F., Weber, P.C., 1999. Crystal structure of the RNA-dependent RNA polymerase from hepatitis C virus reveals a fully encircled active site. *Nat. Struct. Biol.* 6, 937–943.
- Lohmann, V., Korner, F., Herian, U., Bartenschlager, R., 1997. Biochemical properties of hepatitis C virus NS5B RNA-dependent RNA polymerase and identification of amino acid sequence motifs essential for enzymatic activity. *J. Virol.* 71, 8416–8428.
- Lohmann, V., Korner, F., Koch, J., Herian, U., Theilmann, L., Bartenschlager, R., 1999a. Replication of subgenomic hepatitis C virus RNAs in a hepatoma cell line. *Science* 285, 110–113.
- Lohmann, V., Overton, H., Bartenschlager, R., 1999b. Selective stimulation of hepatitis C virus and pestivirus NS5B RNA polymerase activity by GTP. *J. Biol. Chem.* 274, 10807–10815.
- Love, R.A., Parge, H.E., Yu, X., Hickey, M.J., Diehl, W., Gao, J., Wriggers, H., Ekker, A., Wang, L., Thomson, J.A., Dragovich, P.S., Fuhrman, S.A., 2003. Crystallographic identification of a noncompetitive inhibitor binding site on the hepatitis C virus NS5B RNA polymerase enzyme. *J. Virol.* 77, 7575–7581.
- Luo, G., Hamatake, R.K., Mathis, D.M., Racela, J., Rigat, K.L., Lemm, J., Colonna, R.J., 2000. De novo initiation of RNA synthesis by the RNA-dependent RNA polymerase (NS5B) of hepatitis C virus. *J. Virol.* 74, 851–863.
- Lyle, J.M., Bullitt, E., Bienz, K., Kirkegaard, K., 2002. Visualization and functional analysis of RNA-dependent RNA polymerase lattices. *Science* 296, 2218–2222.
- Ma, Y., Shimakami, T., Luo, H., Hayashi, N., Murakami, S., 2004. Mutational analysis of hepatitis C virus NS5B in the subgenomic replicon cell culture. *J. Biol. Chem.* 279, 25474–25482.
- Morin, B., Rahmeh, A.A., Whelan, S.P., 2012. Mechanism of RNA synthesis initiation by the vesicular stomatitis virus polymerase. *EMBO J.* 31, 1320–1329.
- Mosley, R.T., Edwards, T.E., Murakami, E., Lam, A.M., Grice, R.L., Du, J., Sofia, M.J., Furman, P.A., Otto, M.J., 2012. Structure of hepatitis C virus polymerase in complex with primer-template RNA. *J. Virol.* 86, 6503–6511.
- Ng, K.K., Arnold, J.J., Cameron, C.E., 2008. Structure–function relationships among RNA-dependent RNA polymerases. *Curr. Top. Microbiol. Immunol.* 320, 137–156.
- Nomaguchi, M., Ackermann, M., Yon, C., You, S., Padmanabhan, R., 2003. De novo synthesis of negative-strand RNA by Dengue virus RNA-dependent RNA polymerase in vitro: nucleotide, primer, and template parameters. *J. Virol.* 77, 8831–8842.
- O'Farrell, D., Trowbridge, R., Rowlands, D., Jager, J., 2003. Substrate complexes of hepatitis C virus RNA polymerase (HC-J4): structural evidence for nucleotide import and de-novo initiation. *J. Mol. Biol.* 326, 1025–1035.
- Pata, J.D., Schultz, S.C., Kirkegaard, K., 1995. Functional oligomerization of poliovirus RNA-dependent RNA polymerase. *RNA* 1, 466–477.
- Pauwels, F., Mostmans, W., Quiryne, L.M., van der Helm, L., Boutton, C.W., Rueff, A.S., Cleiren, E., Raboisson, P., Surleraux, D., Nyanguile, O., Simmen, K.A., 2007. Binding-site identification and genotypic profiling of hepatitis C virus polymerase inhibitors. *J. Virol.* 81, 6909–6919.
- Perez, A., Marchan, I., Svozil, D., Sponer, J., Cheatham 3rd, T.E., Loughton, C.A., Orozco, M., 2007. Refinement of the AMBER force field for nucleic acids: improving the description of alpha/gamma conformers. *Biophys. J.* 92, 3817–3829.
- Qin, W., Luo, H., Nomura, T., Hayashi, N., Yamashita, T., Murakami, S., 2002. Oligomeric interaction of hepatitis C virus NS5B is critical for catalytic activity of RNA-dependent RNA polymerase. *J. Biol. Chem.* 277, 2132–2137.
- Qin, W., Yamashita, T., Shiota, Y., Lin, Y., Wei, W., Murakami, S., 2001. Mutational analysis of the structure and functions of hepatitis C virus RNA-dependent RNA polymerase. *Hepatology* 33, 728–737.
- Quinkert, D., Bartenschlager, R., Lohmann, V., 2005. Quantitative analysis of the hepatitis C virus replication complex. *J. Virol.* 79, 13594–13605.
- Ranjith-Kumar, C.T., Kao, C.C., 2006. Biochemical activities of the HCV NS5B RNA-dependent RNA polymerase. In: Tan, S.L. (Ed.), *Hepatitis C Viruses: Genomes and Molecular Biology*. Norfolk, UK, pp. 293–310.
- Ranjith-Kumar, C.T., Kim, Y.C., Gutshall, L., Silverman, C., Khandekar, S., Sarisky, R.T., Kao, C.C., 2002. Mechanism of de novo initiation by the hepatitis C virus RNA-dependent RNA polymerase: role of divalent metals. *J. Virol.* 76, 12513–12525.
- Salomon-Ferrer, R., Case, D.A., Walker, R.C., 2013. An overview of the Amber biomolecular simulation package. *WIREs Comput. Mol. Sci.* 3, 198–210.
- Scrima, N., Caillet-Saguy, C., Ventura, M., Harrus, D., Astier-Gin, T., Bressanelli, S., 2012. Two crucial early steps in RNA synthesis by the hepatitis C virus polymerase involve a dual role of residue 405. *J. Virol.* 86, 7107–7117.
- Schmitt, M., Scrima, N., Radujkovic, D., Caillet-Saguy, C., Simister, P.C., Friebe, P., Wicht, O., Klein, R., Bartenschlager, R., Lohmann, V., Bressanelli, S., 2011. A comprehensive structure–function comparison of hepatitis C virus strain JFH1 and J6 polymerases reveals a key residue stimulating replication in cell culture across genotypes. *J. Virol.* 85, 2565–2581.
- Schymkowitz, J., Borg, J., Stricher, F., Nys, R., Rousseau, F., Serrano, L., 2005. The FoldX web server: an online force field. *Nucleic Acids Res.* 33, W382–W388.
- Shi, S.T., Herlihy, K.J., Graham, J.P., Nonomiya, J., Rahavendran, S.V., Skor, H., Irvine, R., Binford, S., Tatlock, J., Li, H., Gonzalez, J., Linton, A., Patick, A.K., Lewis, C., 2009. Preclinical characterization of PF-00868554, a potent nonnucleoside inhibitor of the hepatitis C virus RNA-dependent RNA polymerase. *Antimicrob. Agents Chemother.* 53, 2544–2552.
- Simister, P., Schmitt, M., Geitmann, M., Wicht, O., Danielson, U.H., Klein, R., Bressanelli, S., Lohmann, V., 2009. Structural and functional analysis of hepatitis C virus strain JFH1 polymerase. *J. Virol.* 83, 11926–11939.
- Spagnolo, J.F., Rossignol, E., Bullitt, E., Kirkegaard, K., 2010. Enzymatic and nonenzymatic functions of viral RNA-dependent RNA polymerases within oligomeric arrays. *RNA* 16, 382–393.
- Steitz, T.A., 1999. DNA polymerases: structural diversity and common mechanisms. *J. Biol. Chem.* 274, 17395–17398.
- Tina, K.G., Bhadra, R., Srinivasan, N., 2007. PIC: protein interactions calculator. *Nucleic Acids Res.* 35, W473–W476.
- Vaughan, R., Fan, B., You, J.S., Kao, C.C., 2012. Identification and functional characterization of the nascent RNA contacting residues of the hepatitis C virus RNA-dependent RNA polymerase. *RNA* 18, 1541–1552.
- Waheed, Y., Saeed, U., Anjum, S., Afzal, M.S., Ashraf, M., 2012. Development of global consensus sequence and analysis of highly conserved domains of the HCV NS5B protein. *Hepat. Mon.* 12, e6142.
- Wang, Q.M., Hockman, M.A., Staschke, K., Johnson, R.B., Case, K.A., Lu, J., Parsons, S., Zhang, F., Rathnachalam, R., Kirkegaard, K., Colacino, J.M., 2002. Oligomerization and cooperative RNA synthesis activity of hepatitis C virus RNA-dependent RNA polymerase. *J. Virol.* 76, 3865–3872.
- Wang, W., Kollman, P.A., 2000. Free energy calculations on dimer stability of the HIV protease using molecular dynamics and a continuum solvent model. *J. Mol. Biol.* 303, 567–582.
- Zhong, W., Uss, A.S., Ferrari, E., Lau, J.Y., Hong, Z., 2000. De novo initiation of RNA synthesis by hepatitis C virus nonstructural protein 5B polymerase. *J. Virol.* 74, 2017–2022.